JACS
JOURNAL OF THE AMERICAN CHEMICAL SOCIETY

Communication

pubs.acs.org/JACS

Direct Observation of a Metastable Crystal Phase of Li_xFePO_4 under Electrochemical Phase Transition

Yuki Orikasa,*[,†] Takehiro Maeda,[†] Yukinori Koyama,[‡] Haruno Murayama,[‡] Katsutoshi Fukuda,[‡] Hajime Tanida,[‡] Hajime Arai,[‡] Eiichiro Matsubara,[§] Yoshiharu Uchimoto,[†] and Zempachi Ogumi[‡]

[†]Graduate School of Human and Environmental Studies, Kyoto University, Yoshida-nihonmatsu-cho, Sakyo-ku, Kyoto 606-8501 Japan

[‡]Office of Society-Academia Collaboration for Innovation, Kyoto University, Gokasho, Uji, Kyoto 611-0011, Japan

[§]Department of Materials Science and Engineering, Kyoto University, Yoshida-honmachi, Sakyo-ku, Kyoto 606-8501, Japan

Supporting Information

ABSTRACT: The phase transition between $LiFePO_4$ and $FePO_4$ during nonequilibrium battery operation was tracked in real time using time-resolved X-ray diffraction. In conjunction with increasing current density, a metastable crystal phase appears in addition to the thermodynamically stable $LiFePO_4$ and $FePO_4$ phases. The metastable phase gradually diminishes under open-circuit conditions following electrochemical cycling. We propose a phase transition path that passes through the metastable phase and posit the new phase's role in decreasing the nucleation energy, accounting for the excellent rate capability of $LiFePO_4$. This study is the first to report the measurement of a metastable crystal phase during the electrochemical phase transition of Li_xFePO_4.

Phase transitions of solid-state materials are widely utilized in electronic and electrochemical devices.[1,2] Phase transitions are explained using a phase diagram with physicochemical parameters (e.g., concentration and temperature). Phase diagrams, including the stability of phase transitions, are explained using the concept of Gibbs energy based on the equilibrium between stable phases on either side of a phase transition. For phase transitions in practical devices such as lithium ion batteries (LIBs), the actual phase transition takes place under nonequilibrium conditions, which can result in phenomena different from those expected on the basis of equilibrium thermodynamics. Here we report the experimental investigation of a phase transition in LIBs under nonequilibrium conditions in which a metastable crystal phase was observed as a transient state. To our knowledge, this is the first study to report such an experimental observation of a metastable crystal phase during LIB operation.

Olivine-structured lithium iron phosphate ($LiFePO_4$), which is widely used as a positive electrode material in LIBs,[3] was examined in this study. This material shows a high power density,[4] even though the diffusion of lithium in the material is reportedly quite slow.[5] Understanding the mechanism of the phase transition can be of help in identifying the origin of this fast charge–discharge ability. Under charging and discharging, the material undergoes phase reactions between Li-rich $Li_{1-\alpha}FePO_4$ (LFP) and Li-poor $Li_\beta FePO_4$ (FP).[6] This system is described by a eutectoid-type binary phase diagram.[7,8] However, the LFP–FP phase transition model underlying battery operation has been the subject of debate for a decade. Although phase transition models such as the isotropic shrinkage core[3] and "domino cascade" models have been proposed,[9] these are based on steady-state results. Some researchers have instead tried to measure the dynamic phase transition behavior. Time-resolved X-ray diffraction (XRD) and X-ray absorption spectroscopy measurements indicated a possible time lag in the expected phase transition during electrochemical reactions.[10−12] Theoretical studies and in situ XRD measurements concluded that an undetectable phase is formed during the charge–discharge reaction.[13,14] In addition, recently performed theoretical calculations predicted a single-phase-transition path under nonequilibrium conditions.[15] The phase field simulation suggested dynamic suppression of the phase separation under high currents.[16] Such transient and nonequilibrium phenomena would finish in a short time. Therefore, the mechanism under nonequilibrium conditions remains unclear because of the lack of experimental evidence. In this work, we investigated the dynamics of the phase transition under high-current battery operation using time-resolved XRD, with an emphasis on the transient emergence of a metastable crystal phase between LFP and FP. The phase transition path through the metastable phase can explain the high rate capability of $LiFePO_4$.

Valence changes associated with lithium extraction and insertion inevitably occur under charge–discharge conditions. The phase transition rate is usually controlled electrochemically, whereby the number of electrons moving is fixed galvanostatically. The variation of the electronic charge on Li_xFePO_4 was investigated using X-ray absorption near-edge structure (XANES). XANES spectra acquired during the interconversion of LFP and FP reflect the fraction of divalent and trivalent Fe in the LFP and FP phases, respectively.[10,17] The charge transfer in Li_xFePO_4 almost synchronizes with the electrochemical control (Figure S5 in the Supporting Information). The ideal fraction change from in situ XANES

Received: December 22, 2012
Published: April 1, 2013

   dx.doi.org/10.1021/ja312527x | J. Am. Chem. Soc. 2013, 135, 5497−5500

under conditions of high current density was found to be consistent with a recently reported XANES result.[17]

The crystal phase transition was tracked by time-resolved XRD. The transient state is quite different from the well-known two-phase reaction. Figure 1a shows the changes in the XRD

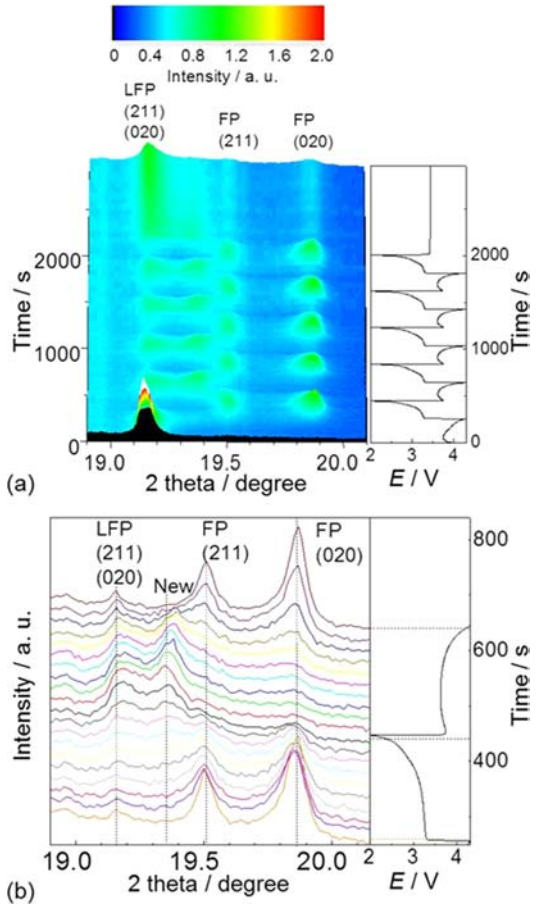

Figure 1. (a) Time-resolved XRD patterns for Li_xFePO_4 during galvanostatic charge−discharge cycles at a rate of 10C. The (211) and (020) diffraction peaks of $LiFePO_4$ at 19.15° overlap, whereas those of $FePO_4$ at 19.50° and 19.87° do not. (b) Detailed XRD patterns during the first discharge and second charge reactions. A new peak at 19.35° clearly appears during cycling. The voltage profiles during the measurements are shown at the right.

peak positions during five charge−discharge cycles at a rate of 10C with a relaxation period between cycles. Before charging, a peak at 19.15° was observed, corresponding to diffraction by the (211) and (020) planes of LFP. The charge reaction causes the appearance of peaks at 19.50° and 19.87°, which are attributable to the (211) and (020) planes of the FP phase, respectively. Very interestingly, in addition to the diffraction peaks due to the thermodynamically expected phases, an unknown peak was detected at 19.35° during the first discharge and subsequent charge−discharge reactions. The appearance of the new peak can be seen more clearly in the individual diffraction patterns acquired during the first discharge and second charge, as shown in Figure 1b.

The new peak was observed between the peaks of LFP and FP in the 2θ range and was formed and disappeared reproducibly in synchronization with the electrochemical cycling. These results suggest that the new peak is related to an olivine-type Li_xFePO_4 phase with an intermediate composition. Although no stable phase between LFP and FP appears in the room-temperature phase diagram, a solid-solution phase forms at temperatures greater than 300 °C.[7,8] Temperature-cycled XRD studies have shown that solid-solution phases such as $Li_{0.75}FePO_4$ and $Li_{0.6}FePO_4$ remain as metastable components even after cooling to room temperature.[8,18] To investigate the crystal structure of the new phase observed in this study in more detail, other crystallographically involved peaks were also analyzed (Figure S6). Following the conclusion of the first discharge reaction, several peaks not assignable to LFP and FP were consistently observed in the other 2θ range, suggesting the presence of a metastable crystal phase. If it is supposed that the new peak at 19.35° is the (020) diffraction peak for the transient Li_xFePO_4 phase, the lattice constants would be a = 10.21 Å, b = 5.945 Å, and c = 4.750 Å. The (211) diffraction peak for the new phase would then be located at 19.18°, overlapping with the (211) and (020) peaks of LFP. On the other hand, if the new peak at 19.35° is the (211) diffraction peak for the new phase, the calculated lattice constants would be a = 10.21 Å, b = 5.725 Å, and c = 4.750 Å, and the (020) diffraction peak would be located at 20.10°. This is unlikely to be the case because the calculated value of b is smaller than that for FP, and no peak was observed at 20.10°. The above lattice constants were estimated from three diffraction peaks. When the peak shift of the new phase was taken into account, b was estimated as 5.936−5.945 Å. According to Vegard's law, this range of lattice constant values corresponds to Li_xFePO_4 (x = 0.61−0.66). The (200) and (301) diffraction peaks also shifted toward higher angles during the charge reaction. It should be noted here that these peaks slightly shifted during electrochemical cycling, yielding some uncertainty in the calculated lattice constants. Despite such uncertainty, the lattice constants are almost consistent with the reported values of thermally formed metastable solid solutions of Li_xFePO_4 with a reported lithium composition of 0.6−0.75.[8,18] Therefore, the new peaks observed during the charge−discharge reaction are believed to derive from an electrochemically formed Li_xFePO_4 (x = 0.6−0.75) solid-solution phase. On the atomic scale, lithium vacancy ordering in partially delithiated $LiFePO_4$ was observed by aberration-corrected annular bright-field scanning transmission electron microscopy (ABF-STEM).[19] The metastable solid-solution phase found in this study might similarly have vacancy ordering on the atomic scale.

The diffraction peak of the new phase disappeared during the relaxation process following the charge−discharge reactions (Figure 1a). This suggests that the presence of the new phase is transient. From the time-dependent decay of the peak area during relaxation, the lifetime of the new phase was estimated to be ∼30 min (Figure S7). The rate dependence of the formation of the new peak would be helpful for further understanding of this point. Figure 2 shows XRD patterns acquired at the end of the first discharge reaction carried out with a range of reaction rates. The XRD pattern for a sample that was allowed to rest for 1 day after 10C charge−discharge is also shown. The new peak was clearly observed for the 10C charge−discharge rate, while the relative peak intensity strongly depended on the rate. After the 1 day relaxation period, the new peak was not observed in any case. This indicates that the new Li_xFePO_4 (x = 0.6−0.75) phase is metastable and rapidly transforms to the stable LFP and FP phases.

The results from in situ time-resolved XRD measurements represent experimental evidence in favor of the existence of a

dx.doi.org/10.1021/ja312527x | J. Am. Chem. Soc. 2013, 135, 5497−5500

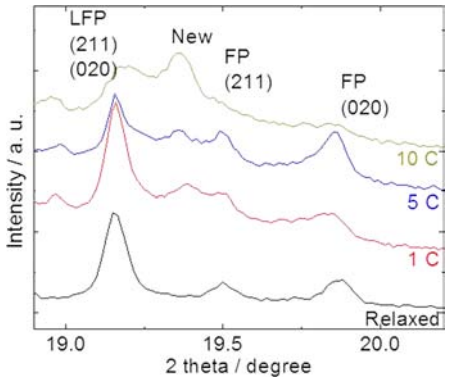

Figure 2. Time-resolved XRD patterns at the end of the first discharge reaction at various charge−discharge rates. "Relaxed" in the figure represents the pattern for a sample that was allowed to relax for 1 day after 10C charge−discharge cycles.

path between FP and LFP that involves a nonequilibrium phase transition. Figure 3 schematically illustrates this observed path along with a path involving a quasi-static phase transition. When the reaction potential of the discharge process is just below the equilibrium potential between the FP and LFP phases, a direct phase transition from FP to LFP should occur (range A in Figure 3b). This situation corresponds to the quasi-static phase transition. The rate-determining step in the phase transition of Li_xFePO_4 is then expected to be the nucleation reaction.[9] The large lattice mismatch between FP and LFP (+3.6% and −1.8% along the *b* and *c* axes, respectively) gives rise to a large interfacial energy. In this case, the quasi-static phase transition can make only a small contribution to the current flux because of the large interfacial energy. A large underpotential would be required for a discharge process with a high current flux, leading to a much lower discharge potential than at equilibrium. Further explanation is provided in Figure S11.

The reaction potential between the FP phase and the Li_xFePO_4 phase is lower than the equilibrium potential between the FP and LFP phases because the Li_xFePO_4 phase is not a thermodynamically stable phase. Theoretical calculations suggested that the potential difference is ∼10 mV.[15] While the quasi-static phase transition is expected under low current flux, an applied electrochemical driving force with a high current flux can overcome this potential difference (range B in Figure 3b). The rate-determining step of the phase transition between FP and LFP is reported to be nucleation of the formed phase.[9] The nucleation energy is given by the change in free energy for the formation of the new phase, the interfacial energy, and the strain energy. The lattice mismatch between the FP and Li_xFePO_4 phases is considerably reduced (+2.5% and −0.66% along the *b* and *c* axes, respectively) compared with the mismatch between the FP and LFP phases. This reduced lattice mismatch may decrease the strain and interfacial energies and thus the nucleation energy. Nucleation of the metastable Li_xFePO_4 phase would then occur more readily, and the fast phase transition between FP and LFP through the metastable phase would be realized. Therefore, the nonequilibrium phase transition path can make a large contribution to the behavior under a high current flux by acting as a bypass route. The existence of a lower-energy transition path in $LiFePO_4$ under nonequilibrium conditions has also been predicted by Monte Carlo[15] and phase field[16] simulations, although these did not consider the metastable Li_xFePO_4 phase. It should be noted that the Li_xFePO_4 phase decomposes to the LFP and FP phases. The metastable phase may be undetectable at lower reaction rates, even if it is actually formed.

In summary, the mechanism of the phase transition of Li_xFePO_4 during LIB operation was investigated using time-resolved XRD measurements. A new crystal phase appears during the charge−discharge reaction, especially at high current fluxes, and disappears under equilibrium conditions. The calculated lattice constants are consistent with thermally formed metastable Li_xFePO_4 (x = 0.6−0.75). This study is the first to report the experimental observation of a phase transition through a metastable phase during nonequilibrium battery operation. Moreover, we propose that the formation of the metastable phase, which decreases the lattice mismatch, dominates the nucleation energy. The phase transition path through the metastable phase contributes to the high-rate performance of the $LiFePO_4$ system. Use of the transient phase of two-phase reaction systems in LIBs electrodes, which enables high-rate charge−discharge, may pave the way for creating indispensable power sources for the future society.

■ ASSOCIATED CONTENT

Supporting Information

Experimental methods, TEM image of $LiFePO_4$, Rietveld analysis of $LiFePO_4$, charge−discharge profiles at various current densities, time-resolved X-ray absorption spectroscopy

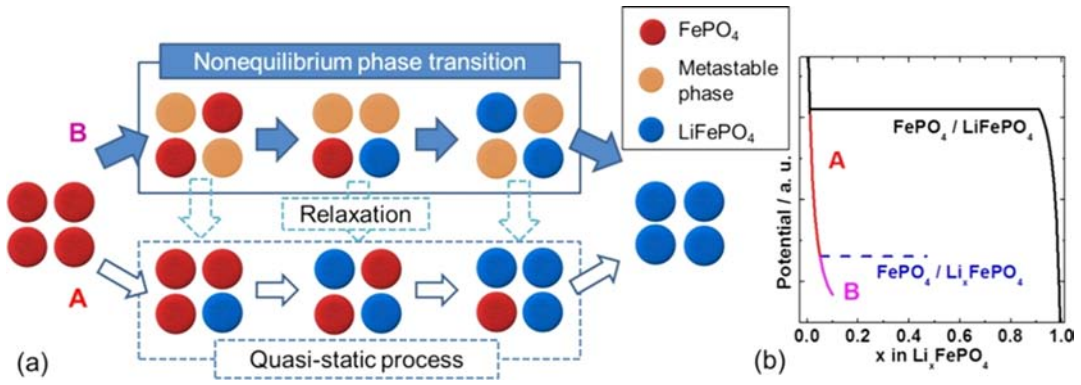

Figure 3. (a) Schematic diagram showing the nonequilibrium phase transition observed experimentally by in situ time-resolved XRD measurements along with a path involving a quasi-static phase transition. (b) Schematic potential profile for Li_xFePO_4. See the text for details regarding ranges A and B in the potential profile.

dx.doi.org/10.1021/ja312527x | J. Am. Chem. Soc. 2013, 135, 5497−5500

analysis, peak analysis of XRD patterns, time-resolved XRD patterns for the (200) and (301) diffractions during 10C charge−discharge reactions, cell design for time-resolved X-ray measurements, and explanation of the chemical potential profiles. This material is available free of charge via the Internet at http://pubs.acs.org.

■ AUTHOR INFORMATION

Corresponding Author
orikasa.yuuki.2a@kyoto-u.ac.jp

Notes
The authors declare no competing financial interest.

■ ACKNOWLEDGMENTS

This work was partially supported by the Research and Development Initiative for Scientific Innovation of New Generation Battery (RISING) Project under the auspices of the New Energy and Industrial Technology Development Organization (NEDO), Japan. The synchrotron radiation experiments were performed at BL01B1, BL28XU, and BL46XU of SPring-8 with the approval of the Japan Synchrotron Radiation Research Institute (JASRI) (Proposals 2012A7601, 2011B1034, 2011B1908, 2011A1014, and 2010B1896).

■ REFERENCES

(1) Wuttig, M.; Yamada, N. *Nat. Mater.* **2007**, *6*, 824.
(2) Winter, M.; Besenhard, J. O.; Spahr, M. E.; Novák, P. *Adv. Mater.* **1998**, *10*, 725.
(3) Padhi, A. K.; Nanjundaswamy, K. S.; Goodenough, J. B. *J. Electrochem. Soc.* **1997**, *144*, 1188.
(4) Kang, B.; Ceder, G. *Nature* **2009**, *458*, 190.
(5) Meethong, N.; Kao, Y. H.; Carter, W. C.; Chiang, Y. M. *Chem. Mater.* **2010**, *22*, 1088.
(6) Yamada, A.; Koizumi, H.; Nishimura, S. I.; Sonoyama, N.; Kanno, R.; Yonemura, M.; Nakamura, T.; Kobayashi, Y. *Nat. Mater.* **2006**, *5*, 357.
(7) Dodd, J. L.; Yazami, R.; Fultz, B. *Electrochem. Solid-State Lett.* **2006**, *9*, A151.
(8) Delacourt, C.; Poizot, P.; Tarascon, J. M.; Masquelier, C. *Nat. Mater.* **2005**, *4*, 254.
(9) Delmas, C.; Maccario, M.; Croguennec, L.; Le Cras, F.; Weill, F. *Nat. Mater.* **2008**, *7*, 665.
(10) Yang, X. Q.; Wang, X. J.; Jaye, C.; Nam, K. W.; Zhang, B.; Chen, H. Y.; Bai, J. M.; Li, H.; Huang, X. J.; Fischer, D. A. *J. Mater. Chem.* **2011**, *21*, 11406.
(11) Leriche, J. B.; Hamelet, S.; Shu, J.; Morcrette, M.; Masquelier, C.; Ouvrard, G.; Zerrouki, M.; Soudan, P.; Belin, S.; Elkaim, E.; Baudelet, F. *J. Electrochem. Soc.* **2010**, *157*, A606.
(12) Chung, K. Y.; Shin, H. C.; Min, W. S.; Byun, D. J.; Jang, H.; Cho, B. W. *Electrochem. Commun.* **2008**, *10*, 536.
(13) Tang, M.; Huang, H. Y.; Meethong, N.; Kao, Y. H.; Carter, W. C.; Chiang, Y. M. *Chem. Mater.* **2009**, *21*, 1557.
(14) Kao, Y. H.; Tang, M.; Meethong, N.; Bai, J. M.; Carter, W. C.; Chiang, Y. M. *Chem. Mater.* **2010**, *22*, 5845.
(15) Malik, R.; Zhou, F.; Ceder, G. *Nat. Mater.* **2011**, *10*, 587.
(16) Bai, P.; Cogswell, D. A.; Bazant, M. Z. *Nano Lett.* **2011**, *11*, 4890.
(17) Yu, X.; Wang, Q.; Zhou, Y.; Li, H.; Yang, X.-Q.; Nam, K.-W.; Ehrlich, S. N.; Khalid, S.; Meng, Y. S. *Chem. Commun.* **2012**, *48*, 11537.
(18) Chen, G. Y.; Song, X. Y.; Richardson, T. J. *J. Electrochem. Soc.* **2007**, *154*, A627.
(19) Gu, L.; Zhu, C.; Li, H.; Yu, Y.; Li, C.; Tsukimoto, S.; Maier, J.; Ikuhara, Y. *J. Am. Chem. Soc.* **2011**, *133*, 4661.